Journal of Alloys and Compounds 495 (2010) 646–649

Contents lists available at ScienceDirect

Journal of Alloys and Compounds

journal homepage: www.elsevier.com/locate/jallcom

Laser remelting of $Al_{91}Fe_4Cr_3Ti_2$ quasicrystalline phase former alloy

P. Gargarella[a,*], R. Vilar[b], A. Almeida[b], C.S. Kiminami[c], C.T. Rios[c], C. Bolfarini[c], W.J. Botta[c]

[a] Programa de Pós-graduação em Ciência e Engenharia de Materiais, Universidade Federal de São Carlos, Rodovia Washington Luiz, Km 235, 13565-905 São Carlos, SP, Brazil
[b] Materials Engineering Department, IST-UTL, Av. Rovisco Pais, 1049-001 Lisbon, Portugal
[c] Departamento de Engenharia de Materiais, Universidade Federal de São Carlos, Rodovia Washington Luiz, Km 235, 13565-905 São Carlos, SP, Brazil

ARTICLE INFO

Article history:
Received 28 July 2008
Received in revised form 26 October 2009
Accepted 27 October 2009
Available online 4 November 2009

Keywords:
Quasicrystal
Laser remelting
Coatings
Al-based alloys

ABSTRACT

In the present work, an Al–Fe–Cr–Ti alloy with adequate composition to form quasicrystalline phases has been surface remelted using laser processing techniques. The surface of spray formed $Al_{91}Fe_4Cr_3Ti_2$ bulk samples was remelted using a 2 kW CW Nd:YAG laser. Two different laser beam powers were applied with the goal of studying its influence in the quasicrystalline phase formation in the remelted coating. After laser treatment, the samples were characterized by X-ray diffractometry (XRD), differential scanning calorimetry (DSC) and scanning electron microscopy (FEG-SEM). The formation of quasicrystalline phases was observed in the X-ray diffractograms and their transformations were verified in DSC analyses. A greater formation of quasicrystalline phase was verified in the coating produced with smaller laser beam power, i.e. higher cooling rate, and its morphology was more close to the sphere. The results indicate the possibility of producing low density coatings containing quasicrystalline phases by laser remelting of spray formed materials.

1. Introduction

Well-ordered and aperiodic quasicrystalline structures including icosahedral and decagonal atomic arrangements [1] provide properties different from conventional structures in metallic materials. Materials with such non-conventional structures exhibit high hardness and stiffness with low fracture toughness and low electrical and thermal conductivities. Although the brittleness restricts their application as bulk engineering materials, their low friction coefficient combined with high hardness directs them to wear resistant material applications, such as in surface cladding of ordinary alloys [2].

A large number of quasicrystalline alloys have been reported, about 80% of them containing aluminum. The most widely investigated systems are those of Al with d-transition metals [3]. In Al-rich alloys, a quasiperiodic structure formed by three-dimensional icosahedral and two-dimensional decagonal quasicrystalline phases is obtained [4].

Many types of nano-quasicrystalline alloys have been developed in the last decades with microstructures consisting of nanometer-sized icosahedral particles embedded in an α-Al solid solution matrix. These alloys present high mechanical strength in comparison to nanocrystalline and commercial Al alloys, maintaining it at high temperatures [5]. However, these nanostructured Al-based alloys are difficult to produce in bulk form due to the high cooling rates necessary during solidification to form the quasicrystalline nanoparticles (10^6 K/s, such as in melt-spinning or atomization processes). Rios et al. [6] studied the formation of quasicrystalline phase in $Al_{92}Fe_3Cr_2Mn_3$ alloy obtained using different methods. They showed that its formation depend on the cooling rate associated in the process, with the larger quasicrystalline phase formation obtained with higher cooling rates.

To reach these rates, rapidly solidification methods must be used, such as spray forming, melting spinning and laser cladding. The high cooling rate in laser cladding [7] makes the process well suited for producing quasicrystalline phases in many alloy coatings on different substrates. The cooling rate obtained during laser surface remelting can be estimated using a model proposed by Ashby and Easterling [8] for a moving hyper point source:

$$\frac{dT}{dt} = -\frac{2\pi\lambda(\Delta T)^2}{\alpha(q*/v)} \text{ and } q* = P_d A\alpha - 2r_b z_m \nu L, \quad (1)$$

where λ is the thermal conductivity, α is the absorptivity at the sample surface, P_d is the power density, A is the area of the laser spot at the surface, v is the scanning speed, ΔT is the range of temperature variation during cooling, r_b is the laser beam radius, z_m is the melt depth, and L is the latent heating of melting. Eq. (1) shows that the cooling rate is inversely proportional to the power applied; a very important parameter for controlling the cooling rate during laser remelting process.

* Corresponding author. Tel.: ++55 16 3351 8549; fax: +55 16 3361 5404.
E-mail addresses: piterg@gmail.com (P. Gargarella), rui.vilar@ist.utl.pt (R. Vilar), amelia.almeida@ist.utl.pt (A. Almeida), kiminami@power.ufscar.br (C.S. Kiminami), triveno@ufmt.br (C.T. Rios), cbolfa@ufscar.br (C. Bolfarini), wjbotta@ufscar.br (W.J. Botta).

0925-8388/$ – see front matter.
doi:10.1016/j.jallcom.2009.10.231

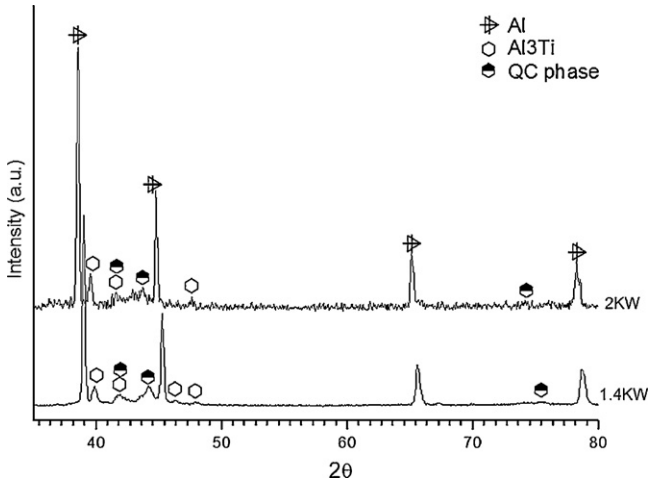

Fig. 1. XRD patterns for coating in the S1 and S2 substrate, refused with power of 2 and 1.4 kW respectively.

Our previous work showed the feasibility of producing coating with quasicrystalline phase formation on a spray formed $Al_{91}Fe_4Cr_3Ti_2$ alloy substrate using the laser remelting technique [9]. Quasicrystalline phase with globular morphology was verified with an estimated volume fraction in the coating of 35%. In this paper the same substrate was used, but now two different laser beam powers were applied for producing remelted coatings, with the goal of studying the influence of different cooling rates in the quasicrystalline phase formation. The samples were analyzed using FEG-MEV, DRX and DSC.

2. Experimental procedure

Two substrates (S1 and S2) with $Al_{91}Fe_4Cr_3Ti_2$ nominal compositions and dimensions of 18 mm × 12 mm × 9 mm and 22 mm × 11 mm × 15 mm, respectively were obtained using the spray-forming process. Their surface was remelted using a 2 kW CW Nd:YAG laser. The laser beam was transported by optical fiber and focused into a spot with a diameter close to 3.05 mm at the surface of the sample. The samples surfaces were sand blasted prior to laser processing in order to clean the surface, achieve uniform roughness and decrease reflectivity.

A coating resulting from overlapping of several individual tracks was made in the S1 substrate. The scanning speed was 100 mm/s and the laser beam power 2 kW. A similar coating was obtained in the S2 substrate with scanning speed of 100 mm/s and 1.4 kW. In both coatings, tracks were overlapped approximately 50% of their width. The nozzle was tilted 17° in relation to the surface normal to avoid back reflection into the laser cavity. The defocusing distance was 10 mm and the track length 22 mm. During the laser treatments the samples were protected by high-purity argon gas atmospheres, either dynamic (substrate S1) with argon flowing in the nozzle output or static (substrate S2) using a box with an argon atmosphere.

The tracks were analyzed by X-ray diffractometry using either a SIEMENS X-ray diffractometer model D-5000 with grazing incidence X-ray (S1 substrate) or a model PW 3710 mpdcontrol PHILIPS X-ray diffractometer (S2 substrate). Cu Kα radiation was used in both diffractometers.

The microstructure of the coatings was characterized by optical microscopy, with an OLYMPUS PMG3 inverted microscope and by scanning electron microscopy (FEG-SEM) using a JEOL 7001F scanning electron microscopy with an Oxford energy dispersive spectrometer (EDS). The thermal stability of the material was studied by differential scanning calorimetry, using a PerkinElmer differential scanning calorimeter (DSC) with an heating rate of 20 K/min (substrate S1) and a Netzsch model 404 DSC with a heating rate of 40 K/min (substrate S2). For the DSC analysis part of the coating including the substrate was cut and the substrate removed by grinding. The samples weights were 10.2 and 16.7 mg for S1 and S2 substrates respectively.

3. Results and discussion

Table 1 shows the laser processing parameters used in the experiments and the resulting track dimensions.

The XRD results are depicted in Fig. 1 for the coating surface in substrate S1 (2 kW) and substrate S2 (1.4 kW). The phases observed

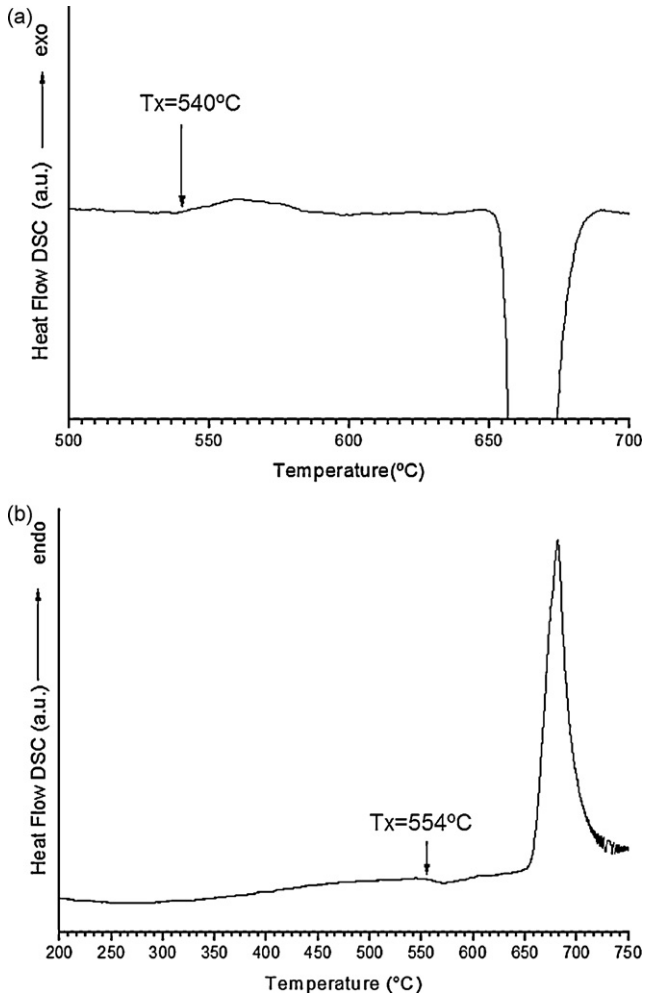

Fig. 2. DSC curves for coatings in the (a) S1 and (b) S2 substrates.

are the same: α-Al, Al_3Ti intermetallic compound and a quasicrystalline icosahedral phase. These same phases were observed by Yamasaki et al. [10] for $Al_{92,5}Fe_{2,5}Cr_{2,5}Ti_{2,5}$ alloy. The QC phase peaks around 42°, 45° and 75° are in agreement with those verified in the literature [11,12]. The peaks are more clear for the coating in the S2 substrate because the analyses were done in a bigger area than for the another sample.

The DSC results for the coatings in substrate S1 and S2 can be observed in Fig. 2. Exothermic peak referents to the quasicrystal–crystal transformation were verified in 540 and 554 °C respectively. These results confirm the presence of quasicrystalline phase in the coating in substrates S1 and S2. This difference in the crystallization temperature occurred because different heating rates were used in the DSC analyses, with 20 and 40 K/min for S1 and S2 substrates respectively. These temperatures are close to that verified by Inoue and co-workers [11], due the transition from the I-phase to $Al_{13}Cr_2 + Al_{13}Fe_4 + Al_{23}Ti_9$ phases.

This high thermal stability of the quasicrystalline phase suggests the use of these alloys in structural applications at high temperatures. Inoue and Kimura [12] verified that this kind of alloy present high strength in elevated temperature that was attributed to the suppression of coarsening of the icosahedral particles and the difficulty of the plastic deformation of the Al phase. Yamasaki et al. [10] showed that a crystallographic relationship between the QC phase and the aluminum matrix phase results in the suppression of the Al-grain coarsening, being responsible for the high strength in elevated temperature.

Table 1
Parameters used and coating dimensions.

Sample	Power density, Pd (W/m^2)	Scanning speedy (mm/s)	Height (mm)	Width (mm)
S1	2.73×10^8	100	0.49	3
S2	1.92×10^8	100	0.25	8.75

The cross-section of the coating in S1 substrate is shown in Fig. 3a. The remelted layer and the as-cast substrate are indicated. Fig. 3b shows the upper region in the coating. The analysis of this microstructure, supported by the EDS/FEG results, allows identifying a dendritic aluminum solid solution matrix with grain boundary precipitates of a phase rich in alloying elements, such as Cr and Fe and another phase consisting of particles with rectangular shape and a composition close to Al_3Ti phase. Another light phase existing in larger proportion with irregular morphology and size between 0.5 and 1 μm can be observed in the aluminum grain boundary. These particles consist probably of the quasicrystalline phase (QC). Its composition obtained by EDS/FEG was $Al_{66}Fe_{18}Cr_{16}$ and probably was affected by the EDS/FEG analysis limitation, taking account of a bigger area than of the QC phase.

A unclear transition between tracks was verified in the cross-section of this coating. Fig. 3c shows a region that probably represents a transition between tracks where the same dendritic aluminum solid solution matrix was observed, with Al_3Ti phase and a small amount of the QC phase. Other intermetallic phases appear with rectangular and hexagonal morphology in large amount.

The cross-section of the coating in the S2 substrate is shown in Fig. 4a. Three regions were verified: the remelted layer, a heat affected zone (HAZ) interlayer and the as-cast substrate. An enlargement of the transition region between remelted layer and the HAZ interlayer can be verified in Fig. 4b. The width of this interlayer is between 30 and 100 μm with the presence of bigger intermetallic phases. Previous studies [9] done in transmission electron microscopy (TEM) showed that this region consist of a mixture of $Al_3(Ti,Cr) + Al_{13}(Fe,Cr)_4$ intermetallic phases precipitated between a-Al fcc submicrometric grains. These phases probably appeared after the decomposition of the QC phase in this thermal affected region during the processing.

Fig. 4c shows the upper region in the coating. Phase with spherical morphology dispersed in a dendritic aluminum matrix can be observed in all the cross-section, with particle size between 0.5 and 1 μm. Previous studies [9] done in TEM showed that this phase corresponds to the QC phase with composition of Al–5.4 ± 0.1Fe–5.5 ± 0.1Cr–2.2 ± 0.1Ti (at.%), very similar to the composition determined by Inoue and co-workers [11]. Its volume fraction is approximately 35%, larger than the volume fraction measured by Yamasaki et al. [10], who obtained only 8% of quasicrystalline phase using a rapid solidification powder atomization method. Another phase, rich in aluminum and iron, was verified in the grain boundaries of the aluminum phase.

A more perfect spherical morphology, normally verified for this phase in aluminum rich alloys [6,10], was found for the QC phases in the coating on S2 substrate. Irregular morphologies as those verified in the coating on S1 substrate can indicate a higher degree of crystallization. The XRD results indicated peaks of QC phase more clear for the coating on S2 substrate, that could occur because of the larger area of analyses or because of the greater presence of this phase in this coating. Another difference between the two coatings is the QC phase composition, with the QC phase obtained in S2 substrate more close to the composition of the QC phases verified in the literature such as $Al_{84.6}Cr_{15.4}$ [13], $Al_{82}Fe_{18}$ [14], $Al_{94}Fe_4Cr_2$ [15] and other quaternary quasicrystals [16] in Al–Fe–Ti–Cr alloys. For explaining these differences two things need to be considered: difference in the oxygen partial pressure and

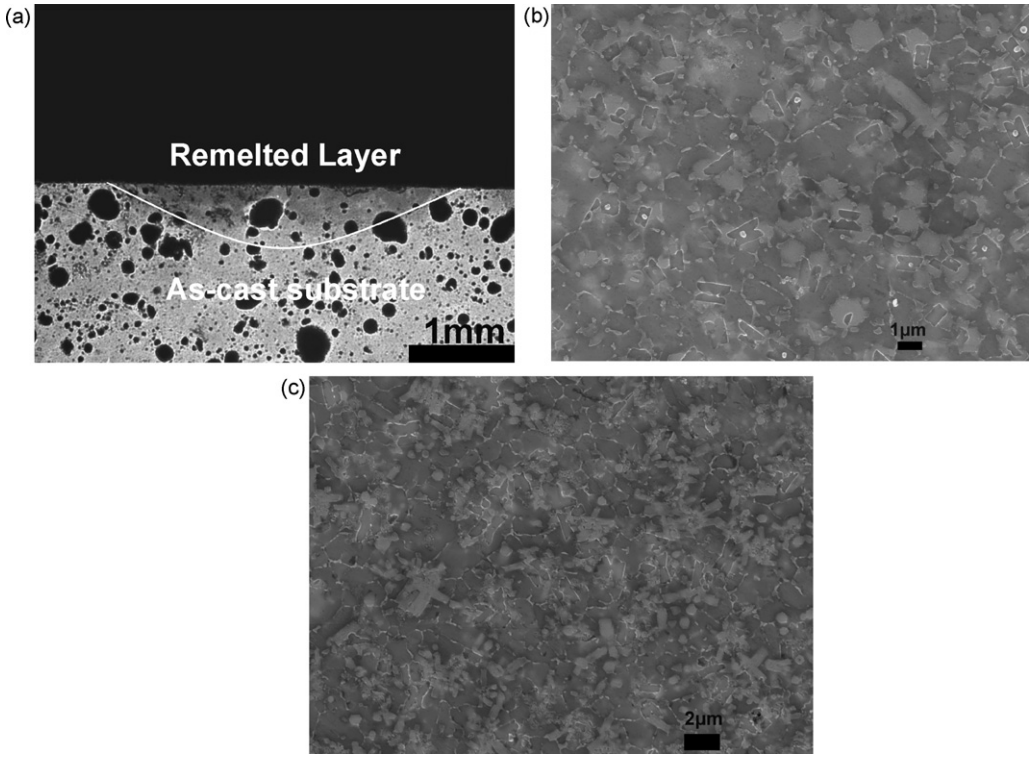

Fig. 3. FEG-MEV micrograph of coating in S1 substrate. (a) Cross-section indicating the remelted layer and the as-cast substrate, (b) upper region in the coating and (c) transition region between tracks.

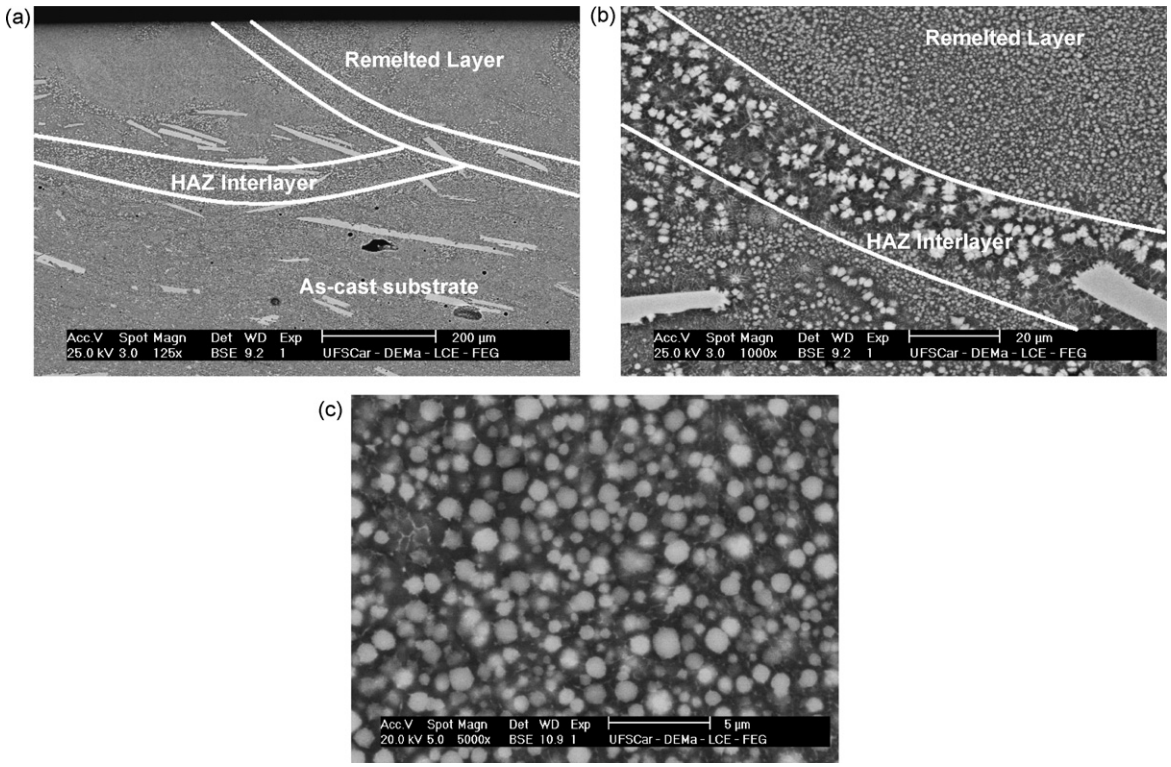

Fig. 4. FEG-MEV micrograph of coating in S2 substrate. (a) Cross-section indicating the remelted layer, heated affected zone (HAZ) interlayer and as-cast substrate, (b) enlargement of the HAZ interlayer and (c) upper region in the coating.

difference in the cooling rate during processing influenced by the porosity.

The difference in the oxygen partial pressure during laser processing could affect quasicrystalline phase formation as well. During solidification, oxide particles may act as heterogeneous nuclei, favoring crystallization of other phases over the QC phase. Considering that the static argon atmosphere in the processing of the S2 substrate provided a lower oxygen partial pressure than that of the S1 substrate, this difference may have affected the quantity of quasicrystalline phases formed, since a larger proportion of quasicrystalline phase was observed in the coating on S2 substrate as compared to S1.

The cooling rate obtained during the processing was calculated using Eq. (1), assuming that the maximum temperature in the melt pool is the melting temperature of the alloy, $\alpha = 0.2$ [17], $\lambda = 243\ \mathrm{W/(m\,K)}$ [18], $L = 390\ \mathrm{kJ/kg}$ [18] and $\Delta T = 825\ \mathrm{K}$ [19]. The calculated cooling rates were -2.75×10^6 and $-3.92 \times 10^6\ \mathrm{K/s}$ for S1 and S2 substrates respectively. These results show that the cooling rate presented the same order of magnitude for both substrates, with a small difference between them. However Figs. 3a and 4a show that a great difference in porosity was verified between them, with the greater porosity for the S1 substrate. This could interfere in the heat extraction of this substrate, which was not considered in the cooling rate calculations, changing this difference.

The substrate used in this experiment, which was obtained by a spray-forming process, presented a homogeneous composition without segregation, which probably improved the quasicrystalline phase formation.

4. Conclusions

The present study showed that it is possible to produce a light alloy coating with quasicrystalline phases by laser remelting of a suitable bulk material.

A greater formation of quasicrystalline phase was verified in the coating produced with smaller laser beam power, i.e. higher cooling rate, and its morphology was more close to the sphere, normally verified for this phase in aluminum rich alloys.

Acknowledgments

This work was supported by FAPESP – Projeto Temático/Brazil, INOV–INESC/Inovação, Portugal and the CAPES/GRICES cooperation program. We are indebted to Mr. Edson Costa dos Santos of IST-UTL/Lisbon for his assistance with the laser processing.

References

[1] P.A. Thiel, Editorial—Progress in Surface Science 75 (2004) 69–86.
[2] R.P. Matthews, C.I. Lang, D. Shechtman, Tribology letters 7 (1999) 179–181.
[3] A.P. Tsai, in: Z. Stadnik (Ed.), Physical Properties of Quasicrystals, Springer, New York, 1999.
[4] B. Grushko, T.Y. Velikanova, Journal of Alloys and Compounds 367 (2004) 58–63.
[5] M. Galano, F. Audebert, B. Cantor, I. Stone, Materials Science and Engineering A 375–377 (2004) 1206–1211.
[6] C.T. Rios, et al., Materials Science and Engineering A 449–451 (2007) 1057–1061.
[7] R. Vilar, Journal of Laser Applications 11 (1999) 64–79.
[8] M.F. Ashby, K.E. Easterling, Acta Metallurgica 32 (1984) 1935–1948.
[9] P. Gargarella, et al., Scripta Materialia 61 (2009) 709–712.
[10] M. Yamasaki, Y. Nagaishi, Y. Kawamura, Scripta Materialia 56 (2007) 785–788.
[11] H.M. Kimura, K. Sasamori, A. Inoue, Journal of Materials Research 15 (2000) 12.
[12] A. Inoue, H. Kimura, Nanostructured Materials 11 (1999) 221–231.
[13] A.P. Tsai, A. Inoue, T. Masumoto, Journal of Materials Science Letters 7 (1988) 322.
[14] E.S.R. Gopal, S. Baranidharan, J.A. Sekhar, Materials Science and Engineering 99 (1988) 413.
[15] R. Manaila, V. Florescu, A. Jianu, A. Badescu, Physica Status Solidi A 109 (1988) 61.
[16] H.M. Kimura, K. Sasamori, A. Inoue, Materials Science and Engineering A 294–296 (2000) 168.
[17] J.F. Ready (Ed.), LIA Handbook of Laser Materials Processing, 182, Magnolia Publishing Inc, 2001.
[18] Metals Handbook, 10th ed., ASM, Metals Park, OH, 1992.
[19] L.F. Bonavina, Processing and Characterization of Rapidly Solidified $Al_{93}Fe_3Cr_2Ti_2$ alloy, Master degree Dissertation, Federal University of São Carlos, Brazil, 2005.